



## Investigation of The Effect of Cr<sub>2</sub>O<sub>3</sub> Particles on Al-Si Matrix Composites Produced by Powder Metallurgy

Serkan ÖZEL<sup>1\*</sup>, Kübra ASLAN<sup>1</sup>

<sup>1</sup>Bitlis Eren Üniversitesi, Mühendislik Mimarlık Fakültesi, Makine Müh. Böl., 13000, Bitlis  
(ORCID: [0000-0003-0700-1295](https://orcid.org/0000-0003-0700-1295)) (ORCID: [0000-0002-9934-1221](https://orcid.org/0000-0002-9934-1221))



**Keywords:** Powder Metallurgy, Metal matrix composite materials, Al, Cr<sub>2</sub>O<sub>3</sub>, Microstructure.

### Abstract

In this study, composite material with Al-12Si (wt%) matrix was produced by powder metallurgy (PM) method. Al-12Si powder was mixed by adding 5, 10 and 15wt% Cr<sub>2</sub>O<sub>3</sub> powder. Al-12Si+ Cr<sub>2</sub>O<sub>3</sub> powder mixture were pressed unidirectional with 500MPa pressure in a cylindrical mold and sintered at 500 °C. After sintering, optical microstructure (OM), Scanning Electron Microscope (SEM), Energy Dispersive Spectrometer (EDS) and microhardness analyzes of the samples were made. When the results were examined, it was observed that a porous structure was formed in all of the samples. Moreover, the lowest hardness was measured in the sample added %15wt Cr<sub>2</sub>O<sub>3</sub> powder sintered at 500 °C.

## 1. Introduction

Metal matrix composites (MMCs) can be formed by the reinforcement added of one or more ceramic particles (for instance: oxide, carbide, boride or others compounds) in a metallic matrix phase. This types composites possess good value of strength and hardness, improved corrosion and wear resistance. Aluminum matrix composites (AMCs), which are generally used for light materials, have high rigidity, enhanced wear and corrosion resistance. AMCs are used in aircraft, automotive and various engineering fields [1-5].

Different primary reinforcements such as SiC, Al<sub>2</sub>O<sub>3</sub>, B<sub>4</sub>C, TiC, MgO are used in the aluminum matrix to produce AMCs. Discontinuously reinforced AMCs are key candidates at light applications as they exhibit high strength, high wear resistance, high hardness and excellent mechanical, physical and thermal properties [2].

Powder metallurgy (PM) is a technology used in the production of high-

strength materials to be used in aerospace, automotive and engineering fields. With this method, composite materials can be produced with the addition of reinforcing particles into the metal matrix that can be heat treated with high strength [6, 7]. Powder metallurgy technique requires a series of processes such as mixing, pressing and sintering of pre-alloyed or pre-mixed powders [8, 9, 10].

The PM method offers several advantages over other MMC manufacturing techniques, such as low processing temperature, low energy consumption and high material usage. In the powder metallurgy process, the reinforcing materials are mixed with the matrix material and compressed at sufficient pressure (depending on the required porosity in the final material). Thereafter, a heating process called sintering is carried out at high temperature (below the melting point of the matrix material) for a sufficient time for diffusion bonding to occur. Compression pressure, sintering temperature and holding time are the parameters that most affect the powder metallurgy process [10, 11, 12].

\*Corresponding author: [sozel@beu.edu.tr](mailto:sozel@beu.edu.tr)

Received: 23.12.2022, Accepted: 19.03.2023

Chromium oxide ( $\text{Cr}_2\text{O}_3$ ) is a hexagonal crystal with a melting point of 2435 °C and it has a Vickers hardness of 1825 HV.  $\text{Cr}_2\text{O}_3$  is commonly known as a catalyst, but it also exhibits high abrasive properties and is therefore widely used in the form of polishing pastes. It is an important refractory material with its high melting temperature and oxidation resistance at high temperatures [13, 14].

In this study, %5, %10 and %15wt  $\text{Cr}_2\text{O}_3$  powders were added to Al-12Si powder as reinforcement. Then, the samples were pressed and sintered at 500 MPa and 500 °C, respectively. After these processes, the effect of reinforcement particle was investigated.

## 2. Material and Method

In this study, Al-12Si powder was used as matrix material. Al-12Si powder is a standard powder produced by gas atomization in the size of  $-90 +45 \mu\text{m}$  by Metco-Oerlikon company. 5, 10 and 15wt%  $\text{Cr}_2\text{O}_3$  powder ( $-35 +15 \mu\text{m}$  by Metco-Oerlikon company, 99.8% purity) was added to the Al-12Si powder mixture as reinforcement material. For the homogeneous distribution of the powders, the mixing process was carried out at a speed of 45 rpm for 45 minutes. The prepared mixtures are given in Table 1.

**Table 1.** Powder mixing ratios of the samples.

Sample No.	Powder (wt%)	$\text{Cr}_2\text{O}_3$ Powder (wt%)
1	100	0
2	95	5
3	90	10
4	85	15

The mixed powder were cold pressed unidirectional at 500 MPa pressure. The pressed samples were sintered for 60 minutes at 500 °C in the Protherm brand heat treatment furnace



**Figure 1.** Heat treatment furnace.

After sintering, the samples were grinded with abrasives with different surface roughness, polished and then etched, for metallographic characterization. A mixture of 95 ml  $\text{H}_2\text{O}$ , 1 ml of HF, 2.5 ml of  $\text{HNO}_3$  and 1.5 ml of HCl was used as etchant. Etching was carried out for 30-35 seconds. Afterward, the microstructural examination were carried out with Nikon brand optical microscope (Figure 2) in Yahya Eren Advanced Research Laboratory of Bitlis Eren University.



**Figure 2.** Optical microscope

Scanning electron microscope (SEM) and EDS analyzes were performed for microstructure characterization of samples. Hardness measurements were taken with Qness Q10M brand microhardness device (Figure 3). Phase analyzes of the samples were performed on the Rigaku brand RadB model XRD device.

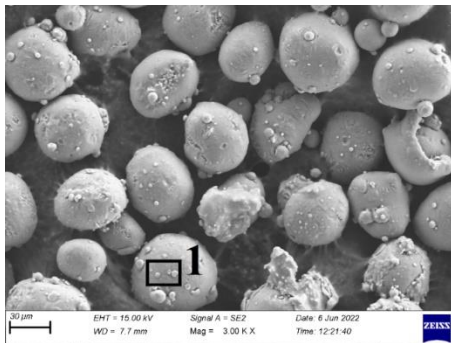


Figure 3. Microhardness tester.

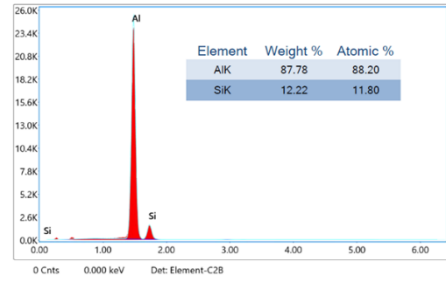
### 3. Results and Discussion

#### 3.1. Microstructure Analysis of the Samples

Figure 4 shows the SEM pictures and EDS analysis of the pre-alloyed Al-12Si powder.



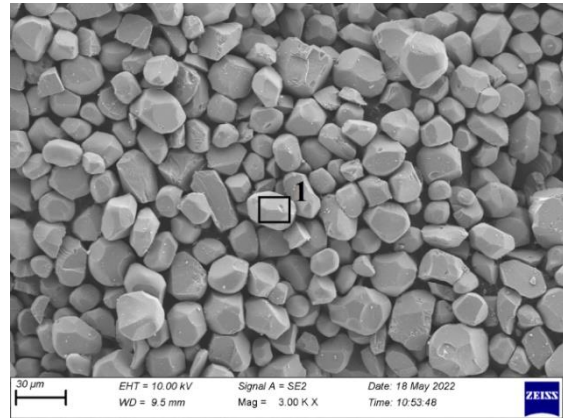
(a)



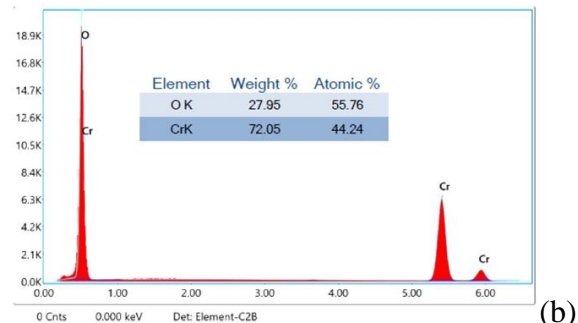
(b)

Figure 4. a) SEM photograph taken from Al-12Si powder, b) EDS analysis taken from area 1 in Figure 3 a.

In the EDS analysis taken from area 1 in Figure 4a, the presence of Al element and Si element can be seen (see Figure 4b). Al-12Si powder is a pre-alloyed powder containing 12% Si. According to the EDS analysis, 12.22% Si element was detected in the Al element.



(a)

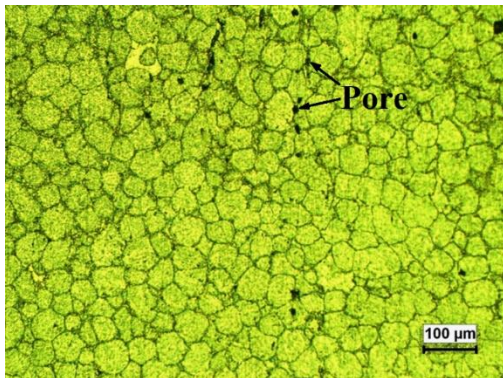


(b)

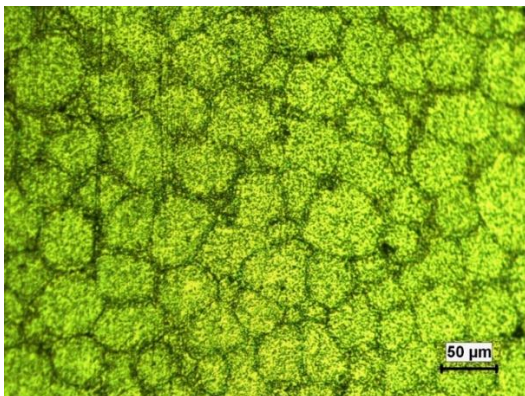
Figure 5. a) SEM photograph taken from Cr<sub>2</sub>O<sub>3</sub> powder, b) EDS analysis of Cr<sub>2</sub>O<sub>3</sub> powder taken from area 1 in Figure 4 a.

Figure 5 shows the SEM pictures and EDS analysis of the  $\text{Cr}_2\text{O}_3$  powder. The presence of Cr and O elements can be seen from the results of the EDS analysis of  $\text{Cr}_2\text{O}_3$  powder shown in Figure 5b. In the EDS analysis, a percentage of 72.05% Cr and 27.95% O element were determined. Therefore, it can be said that the Cr and O elements and the oxide compound (such as  $\text{Cr}_x\text{O}_y$ ) are present.

In Figure 6, optical microstructure pictures of sample 1 are shown. Grain boundaries are clearly visible in the microstructure. It is seen that there are pores in the structure consisting of equiaxed grains. Porosity is inevitable in samples produced with powder metallurgy for reasons such as purity of powders used, mixing ratio of powders, compression pressure and speed [15]. Figure 6 shows the pores located at the grain boundaries.



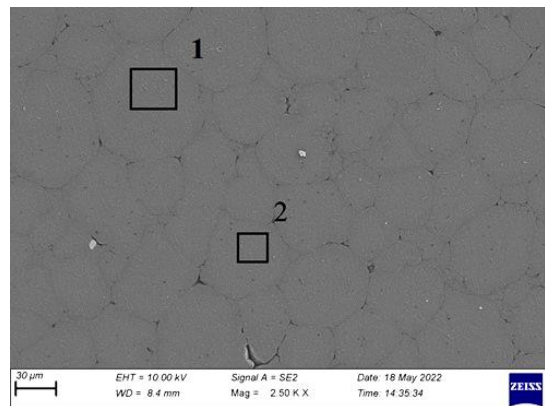
(a)



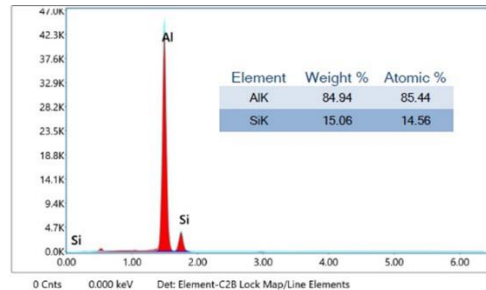
(b)

**Figure 6.** Optical microstructure pictures of the sintered sample 1.

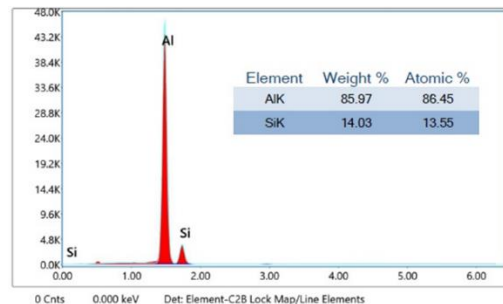
SEM photograph and EDS analysis results taken from sample 1 are shown in Figure 7. Al-Si eutectic structures are thought to be present in the grain and grain boundaries. It is seen that 84.94% Al and 15.06% Si elements are present in area 1 according to EDS analysis (Figure 7a and b). As a result of this EDS, area 1 is thought to be composed of intermetallic compounds with Al-Si eutectic structure. In addition, it is also assumed that the Al-Si eutectic structure is present at a certain percentage in area 2 as a result of the EDS analysis (Figure 7a and c).



(a)



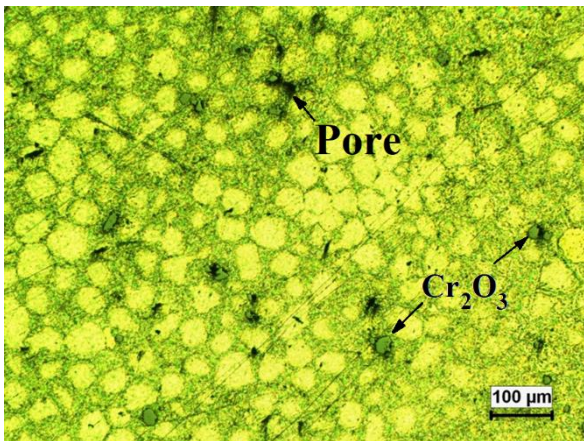
(b)



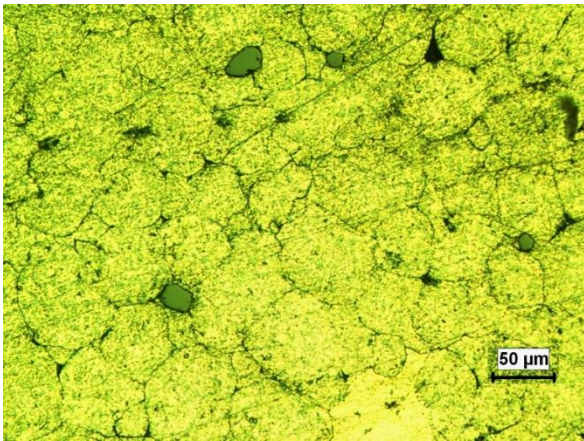
(c)

**Figure 7.** a) SEM photograph, b) EDS analysis area 1 c) EDS analysis area 2 taken from the sintered sample 1

In Figure 8, optical microstructure pictures of the sample 2 are shown. Grain boundaries are seen in the microstructure of the sample. It is thought that there are intermetallic compounds with Al-Si eutectic structure at the grain and grain boundaries of the microstructure consisting of equiaxed grains. It can also be seen that there are pores in black color at the grain boundaries. The sample 2 which possess 5wt%  $\text{Cr}_2\text{O}_3$  compound + 95wt% Al-Si possesses more pores in comparison to the sample 1.



(a)

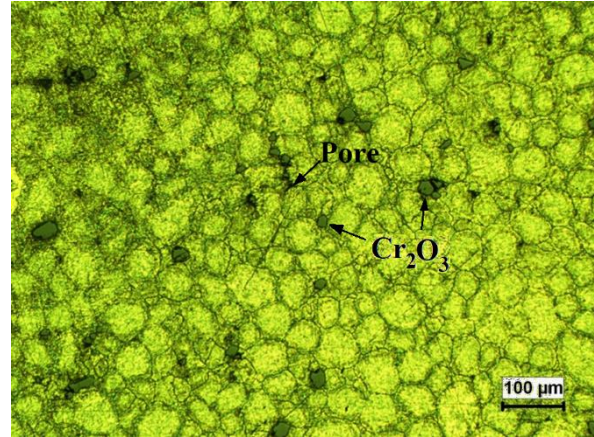


(b)

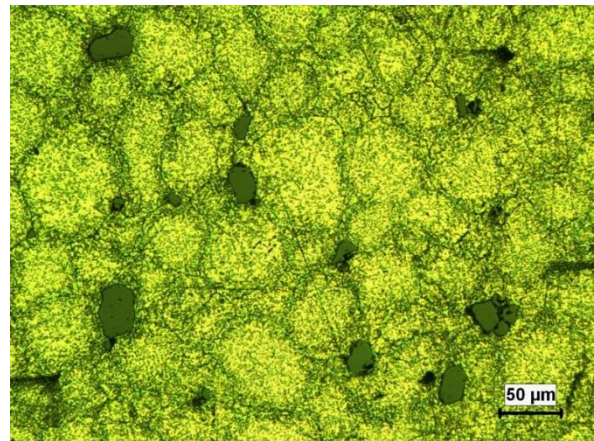
**Figure 8.** Optical microstructure pictures of the sintered sample 2.

Optical microstructure pictures of sintered sample 3 are shown in Figure 9. Grain boundaries can also be seen in the microstructure of this sample. There is similar structure compared to the sample 2 such as the Al-Si eutectic structure is

present in the grain and grain boundaries. 10wt%  $\text{Cr}_2\text{O}_3$  powder added into the Al-Si matrix structure exhibits a homogeneous distribution in the sample 3 (see Figure 9). Partial porosity can also be seen in the microstructure.



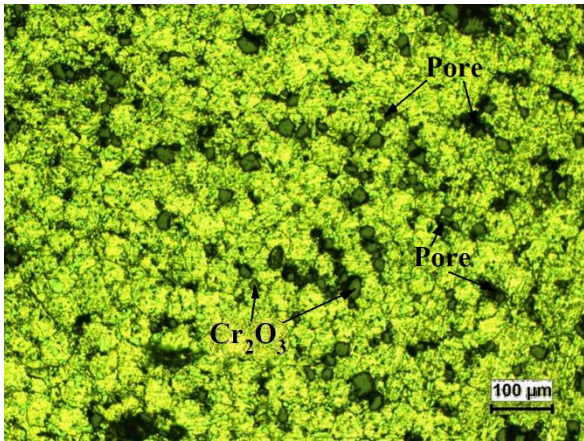
(a)



(b)

**Figure 9.** Optical microstructure pictures of the sintered sample 3.

In Figure 10 shows the optical microstructure pictures of the sample 4. In this sample, grain boundaries are seen in the microstructure. The porosity increased considerably with the addition of 15wt%  $\text{Cr}_2\text{O}_3$  into the Al-Si matrix structure. Al-Si eutectic structure intermetallic compounds are observed in grain boundaries and grain interiors. It can also be seen that the amount of pores around the added  $\text{Cr}_2\text{O}_3$  is more concentrated (see Figure 10).



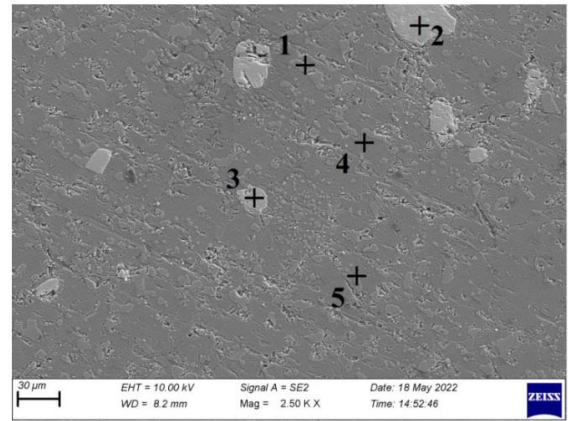
(a)

(b)

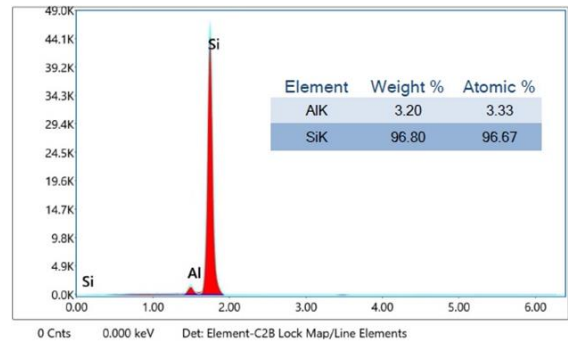
**Figure 10.** Optical microstructure pictures of the sintered sample 4.

SEM photograph and EDS analysis results taken from sample 4 are shown in Figure 11. EDS analyzes were taken from matrix structure, grain boundaries and powder particles. The presence of Al and Si elements is seen in the EDS analysis given in Figure 11-b, taken from the light gray area 1. It is seen that area 1 is rich in Si element with 96.80% Si value and Al matrix element is present with a value of 3.20%. It is understood that there is no oxidation in this area.

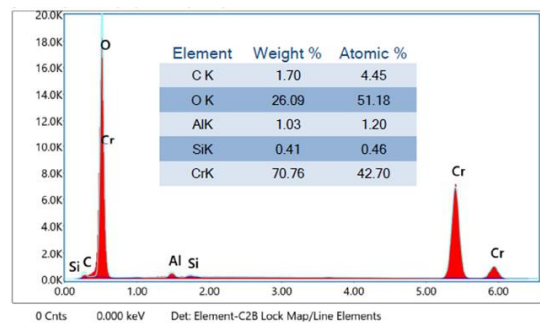
According to EDS analyses taken from point 2 and 3, Cr, Si, Al and O elements are present in these locations (see Figure 11-c and d). It is assumed that both places are composed of Cr<sub>2</sub>O<sub>3</sub> compound. There is a small amount of Al and Si elements, which are matrix structures. It is believed that the element C detected in point 2 comes from the carbon tape used while sticking the samples and powders during the SEM analysis. In the EDS analysis taken from point 4 (see Figure 11-e), it is seen that the Al element has a high value of 99.43%. In addition, a small amount of Si element (0.57%) was detected at this location. 67.4% Si, 24.13% Al and 8.47% O elements were detected in the EDS analysis taken from point 5 (see Figure 11-f). At this point, it is thought that the powders in the matrix structure are oxidized.

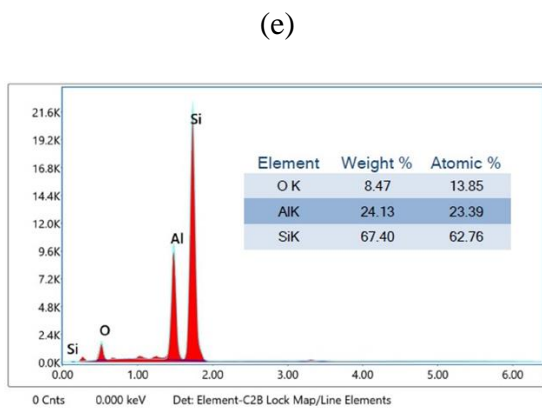
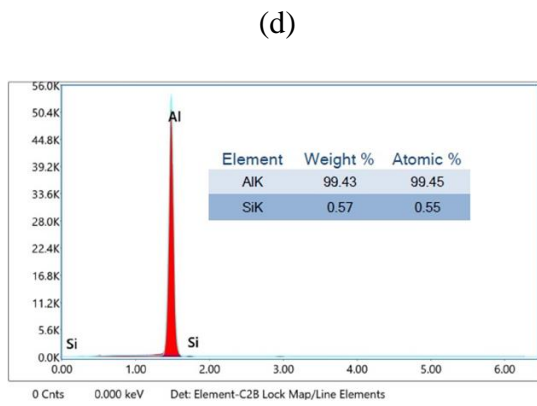
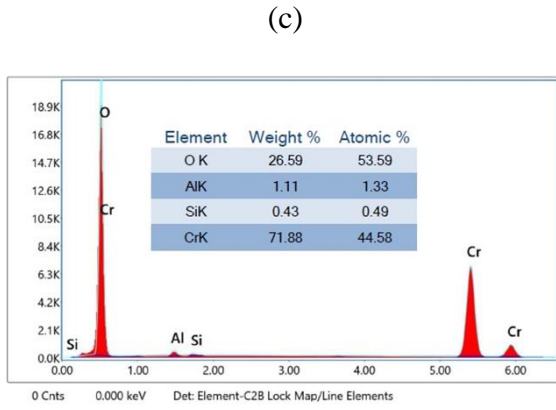


(a)



(b)





(f)

**Figure 11.** a) SEM photograph taken from the sample 4. EDS analysis of the sample 4 taken from b) point 1, c) point 2, d) point 3, e) point 4, and f) point 5 shown in Figure 11a.

XRD analysis of the sample 4 is shown in Figure 12. As a result of XRD analysis, it was determined that different types of compounds were formed.

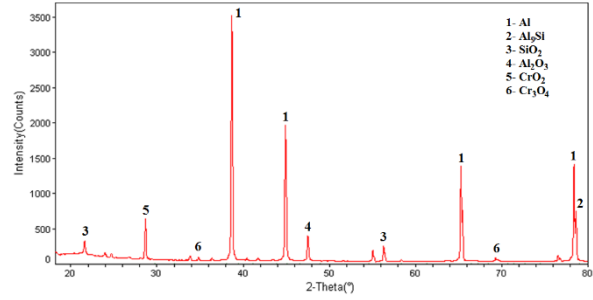


**Figure 12.** XRD analysis of sample 4.

The main phase was determined as Al matrix. In addition,  $Al_9Si$ ,  $Al_2O_3$ ,  $CrO_2$  and  $Cr_3O_4$  compounds were formed depending on the  $Cr_2O_3$  addition. Moreover, it was observed that the elements detected in the EDS analyzes (Figure 11) taken from the sample 4 and the compounds detected in the XRD analysis (Figure 12) taken from the same sample matched.

### 3.2. Microhardness Test Results

The microhardness values of the samples with and without the addition of  $Cr_2O_3$  powder after sintering are given in Figure 13.

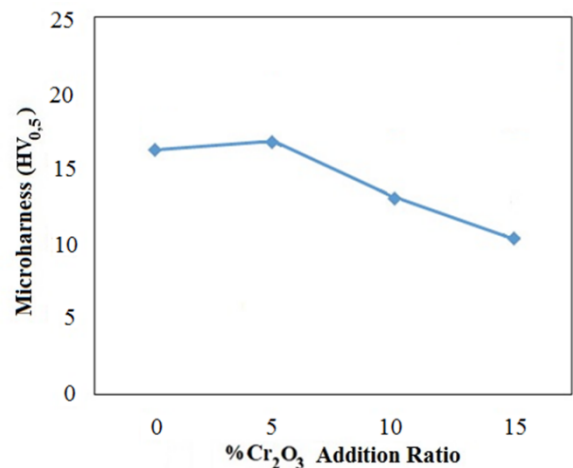


**Figure 13.** Microhardness values of the samples after sintering.

The microhardness value of the sample 1, which has no addition of  $Cr_2O_3$ , was measured as 16,19 HV. Adding %5wt  $Cr_2O_3$  compound into the Al-Si matrix resulted in 16,8 HV. However, increasing the amount of

Cr<sub>2</sub>O<sub>3</sub> from %5wt to %10wt caused the micro hardness to decrease from 16,19 HV to 13,15 HV, respectively. In the sample 4 with 15% Cr added, the hardness was measured as 10,33 HV. With the addition of Cr<sub>2</sub>O<sub>3</sub> powder, the pore partly increased in the microstructure as seen in the microstructure photographs (Figures 8, 9, 10). The highest number of pores was detected in the sample 4 to which %15wt Cr<sub>2</sub>O<sub>3</sub> was added. In powder metallurgy manufacturing, the formation and growth of sintering necks is mainly driven by surface diffusion. The high amount of oxide makes it difficult to neck [17]. It can be said that the amount of pores increases with decreasing necking. Due to this increase in the amount of pores, a small decrease in the amount of microhardness was detected.

#### 4. Conclusion and Suggestions

1. A porous structure was detected in the samples. The pores become more prominent at the grain boundaries. Cr<sub>2</sub>O<sub>3</sub> powders are also located in the grain boundaries.
2. After sintering, the microhardness value of the samples decreased partially due to the

increase in the amount of pores with the addition of Cr<sub>2</sub>O<sub>3</sub> powder.

3. The lowest microhardness value after sintering was found in the %15wt Cr<sub>2</sub>O<sub>3</sub> added sample 4 with an HV value of 10,33.

#### Acknowledgment

Part of this article was presented as a summary paper at the "2<sup>st</sup> International Rahva Technical And Social Researches Congress" congre.

#### Contributions of the authors

This study is a part of Kübra ASLAN's master thesis.

#### Conflict of Interest Statement

There is no conflict of interest between the authors.

#### Statement of Research and Publication Ethics

The study is complied with research and publication ethics.

#### References

- [1] M. Yadav, L. A. Kumaraswamidhas, and S. K. Singh, "Investigation of solid particle erosion behavior of Al-Al<sub>2</sub>O<sub>3</sub> and Al-ZrO<sub>2</sub> metal matrix composites fabricated through powder metallurgy technique," *Tribol. Int.*, vol. 172, no. 107636, p. 107636, 2022.
- [2] K. C. Nayak, P. R. Deshmukh, A. K. Pandey, P. Vemula, and P. P. Date, "Microstructural, physical and mechanical characterization of grinding sludge based aluminium metal matrix composite," *Mater. Sci. Eng. A Struct. Mater.*, vol. 773, no. 138895, p. 138895, 2020.
- [3] I. Bahaj, M. Kaddami, A. Dahrouch, N. Labjar, and M. Essahli, "The effect of particle content and sintering time on the properties of Al-Al<sub>9</sub>Co<sub>2</sub>-Al<sub>13</sub>Co<sub>4</sub> composites, made by powder metallurgy," *Mater. Today*, vol. 62, pp. A1-A7, 2022.
- [4] M. Ardestani and F. Karpasand, "Chemical synthesis and densification of a novel Ag/Cr<sub>2</sub>O<sub>3</sub>-AgCrO<sub>2</sub> nanocomposite powder," *Sci. Eng. Compos. Mater.*, vol. 25, no. 4, pp. 739-743, 2018.
- [5] O. Adıyaman, "Investigation of Mechanical Properties of Composite Al6061/Ni-Al<sub>2</sub>O<sub>3</sub> Produced by Stir Casting Process", *European Journal of Technique (EJT)*, vol. 12, no. 1, pp. 30-35, 2022.
- [6] H. Su et al., "Research on high-temperature mechanical properties and microstructure of powder metallurgical rhenium," *Int. J. Refract. Hard Met.*, vol. 106, no. 105861, p. 105861, 2022.
- [7] M. Boz ve A. Kurt, "Toz metal fren balata malzemelerinin sürtünme-aşınma performansı üzerine çinkonun etkisi," *Mühendislik Mimarlık Fakültesi Dergisi*, vol. 21, no 1, p. 115-121, 2006.
- [8] K. Köprülü, N. Mutlu, A. Kurt, B. Gülenç, Y. Özçatalbaş, "Al+%4,5 Cu ön karışimli tozların alaşımlanmasına ısıl işlemlerin etkisi," *Gazi Uni. J. of Sci. Part C: Des. and Tech.*, vol. 6, no 2, p. 283-293, 2018.

- [9] Y. Sayan, J.-S. Kim, and H. Wu, “Residual stress measurement of a single-step sintered planar anode supported SC-SOFC using fluorescence spectroscopy,” *Bitlis Eren Üniversitesi Fen Bilimleri Dergisi*, vol. 11, no. 3, pp. 902–910, 2022.
- [10] M. Kılıç, I. Kırık, M. Okumus, “Microstructure examination of functionally graded NiTi/NiAl/Ni<sub>3</sub>Al intermetallic compound produced by self-propagating high-temperature synthesis,” *Kovove Mater.*, vol. 55, no 2, pp. 97–106, 2017.
- [11] N. Kumar, A. Bharti, and K. K. Saxena, “A re-investigation: Effect of powder metallurgy parameters on the physical and mechanical properties of aluminium matrix composites,” *Mater. Today*, vol. 44, pp. 2188–2193, 2021.
- [12] Ş. Çetinkaya, “Karbon katkılı alaşımlı demir tozu peletlerinin sinterleme sonrası özellikleri,” M.S. thesis, İstanbul Univ. Graduate Sch. of Nat. and App. Sci., İstanbul, Türkiye, 2005.
- [13] Y. Sayan, V. Venkatesan, E. Guk, H. Wu, and J.-S. Kim, “Single-step fabrication of an anode supported planar single-chamber solid oxide fuel cell,” *Int. J. Appl. Ceram. Technol.*, vol. 15, no. 6, pp. 1375–1387, 2018.
- [14] E. Gevorkyan, L. Cepova, M. Rucki, V. Nerubatskyi, D. Morozow, W. Zurowski, V. Barsamyan and K. Kouril, “Activated sintering of Cr<sub>2</sub>O<sub>3</sub>-based composites by hot pressing”, *Mater.* , vol. 15, pp. 5960, 2022.
- [15] K. Aslan, “Toz metalurjisi yöntemiyle Al+Si matrisli kompozitlerin aşınma dayanımlarının incelenmesi,” M.S. thesis, Bitlis Eren Univ. Inst. of Graduate Edu., Bitlis, Türkiye, 2022.
- [16] M. Kılıç, “Toz metalurjisi ile Üretilen NiTi Alaşımına Al’un Etkisi,” *Bitlis Eren Üniversitesi Fen Bilimleri Dergisi*, vol. 10, no. 1, pp. 256-267, 2021.
- [17] H. He, J. Lou, Y. Li, H. Zhang, S. Yuan, Y. Zhang, X. Wei, “Effects of oxygen contents on sintering mechanism and sintering-neck growth behaviour of FeCr powder,” *Powder Techn.*, vol. 329, pp. 12-18, 2018.